Supporting Information

Densely Populated Tiny RuO$_2$ Crystallites Supported by Hierarchically Porous Carbon for Full Acidic Water Splitting

Bo Yu,[1,2] Jin-Hang Liu,[3] Shuaibiao Guo,[1] Guanlin Huang,[4] Shengjia Zhang,[5]

Shuangqiang Chen,[1] Xiaopeng Li,*[4] Yong Wang,*[1,2] and Li-Ping Lv,*[1,2]

[1]*Department of Chemical Engineering, School of Environmental and Chemical Engineering, Shanghai University, 99 Shangda Road, Shanghai, P. R. China, 200444*

[2]*Key Laboratory of Organic Compound Pollution Control Engineering (MOE) Shanghai University, 99 Shangda Road, Shanghai, P. R. China, 200444*

[3]*School of Chemistry and Chemical Engineering, Jiangxi Province Engineering Research Center of Ecological Chemical Industry, Jiujiang University, Jiujiang 332005, China*

[4]*College of Materials Science and Engineering, Donghua University, 2999 North Renmin Road, Shanghai, P. R. China, 201620*

[5]*School of Mechanical Engineering, Energy and Power Engineering program, Shanghai JiaoTong University, 800 Dongchuan Road, Shanghai, P.R. China, 200240*

*Corresponding authors: Tel: +86-21-66137723; fax: +86-21-66137725.

Email address: liping_lv@shu.edu.cn; xiaopeng.li@dhu.edu.cn;

yongwang@shu.edu.cn;

Experimental Section

Materials: Polyacrylamide (PAM, 90%) was purchased from Tianjin Yuanli Chemical. Sodium nitrate (NaNO$_3$, 99%) was purchased from Sinopharm Holding. Ruthenium chloride hydrate (RuCl$_3 \cdot$xH$_2$O,) was purchased from Aladdin. The water used in the experiments was deionized water (18.2 MΩ, Milli-Q pores).

Preparation of PC: Polyacrylamide (0.5 g) and sodium nitrate (0.1 g) were first mixed with a mass ratio of 5:1. Then 20 ml of ionized water was added followed with an ultrasonic treatment for 2 hours. Thereafter, the dispersion was freeze-dried and then mashed into a white powder with a mortar. Finally, the powder samples were calcined

at 700 °C for 2 hours with a heating rate of 5 °C/min in N_2 atmosphere to obtain black bulk samples. Then the collected products were soaked in deionized water for 24 hours, filtered and dried to obtain the final porous carbon powder, which was denoted as PC.

Preparation of RuO2/PC: The as-prepared porous carbon (PC, 25 mg) and $NaNO_3$ (1000 mg) were added to a quartz beaker, mixed well and then transferred to a muffle furnace followed with heating at 350 °C for 20 min. When the $NaNO_3$ was melted, 10 mg of $RuCl_3 \cdot xH_2O$ was added to the quartz beaker. After 5 min, the quartz beaker was removed from the muffle and cooled to room temperature. After cooling, the samples were placed in deionized water and soaked for 6 hours, then the samples were cleaned by extraction. Finally, the product was redispersed in 5 mL of deionized water and freeze-dried in vacuum. The product obtained is designated as RuO_2/PC-0.4, where 0.4 represents the mass feeding ratio of $RuCl_3 \cdot xH_2O$ to PC.

For comparison, RuO_2/PC-1 and RuO_2/PC-0.25 were also prepared (same as the synthesis method of RuO_2/PC-0.4, with only the mass feeding ratio of $RuCl_3 \cdot xH_2O$ to PC changed, namely 1:1 and 0.25:1). At the same time, a PC-free RuO_2 sample was also directly synthesized (same as the synthesis method of RuO_2/PC-0.4, except that PC was not added in the first step).

Characterizations: Transmission/scanning electron microscope (TEM/SEM, JEM-F200(URP)/JSM-6700F), X-ray powder diffractometer (XRD, D8 Advance) were used to characterize the morphology, structure and chemical composition of the product. The composition and chemical/electronic states of the elements in the product were characterized on an X-ray photoelectron spectrometer (XPS, Thermo Scientific K-Alpha). The content of Ru element in the products was analyzed with an inductively coupled plasma-optical emission spectrometer (ICP-OES, Optima 2100DV). Finally, the specific surface area, pore size and distribution of the materials were examined with an automatic surface and porosity analyzer (Micromeritics, ASAP 2460). The X-ray absorption fine structure (XAFS) measurements were performed on the beamline BL14W1 in the Shanghai Synchrotron Radiation Facility (SSRF) with the electron storage ring operated at 3.5 GeV, equipped with a double Si (111) crystal monochromator. The data were obtained at transmission mode and analyzed using the IFEFFIT software package.

Electrochemical Measurements:

Preparation of catalyst ink: The catalyst ink was prepared by adding 50 μL of Nafion solution, 200 μL of ultrapure water, and 750 μL of isopropanol to 5 mg of the prepared sample, respectively, and then sonicated for 60 min. Electrochemical measurements were all performed on a CHI 660E electrochemical workstation (Shanghai Chenhua, China). The catalytic performance of the samples for HER and OER at room temperature was investigated in a three-electrode system containing 0.5 M H_2SO_4 solution. A 1 × 2 cm rectangular carbon paper, a Pt mesh and an Ag/AgCl (3 M KCl) electrode were respectively used as the working, counter and reference electrode. 50 μL of the above catalyst ink was evenly spreading on the 1 × 1 cm area of the carbon paper with a pipette. The catalyst loading on carbon paper was around 25 mg cm^{-2}.

For the OER tests, the electrochemical potential measured on the Ag/AgCl reference electrode was converted to a reversible hydrogen electrode (RHE) scale according to the Nernst equation: $E_{RHE}= E_{Ag/AgCl}+ 0.059pH + 0.197$

Note that the Ag/AgCl reference electrode used for the HER tests was supposed to deviate from standard due to aging. Therefore, to obtain an accurate potential of the aging reference electrode, a three-electrode system in 0.5M H_2SO_4 with a brand-new Ag/AgCl as reference electrode, a Pt net as counter electrode and the aging Ag/AgCl electrode that was previously used for HER test as the working electrode, was constructed. Then the open-circuit potential was recorded on a CHI 760 electrochemical workstation to detect the potential deviation (ΔV) of the aging reference electrode from the standard Ag/AgCl electrode. To covert the measured potentials to RHE scale, the following equation $E_{RHE}= E_{Ag/AgCl}+ 0.059\ pH + 0.197+\Delta V$ was adopted, in which ΔV was tested to be 0.0871V.

Cyclic voltammetry (CV) activates the active material on the working electrode, and then linear sweep voltammetry (LSV) is performed to obtain the polarization curves of the above samples. For the OER test, CVs were first recorded in 0.5 M H_2SO_4 solution at a scan rate of 100 mV s^{-1} with potentials ranging from 0.8 to 1.5 V for 100 consecutive cycles. Then, LSV was performed in the same potential range at a scan rate of 5 mV s^{-1} without IR compensation. For HER activity investigation, CVs were

recorded in 0.5 M H_2SO_4 solution at a scan rate of 100 mV s^{-1} at potentials ranging from 0 to −0.4 V for 100 consecutive cycles. Then, LSV was performed at a scan rate of 5 mV s^{-1} over the same potential range without compensation. Electrochemical impedance spectroscopy (EIS) was performed from 100 kHz to 0.01 Hz with alternating current (AC) amplitude of 5 mV for OER at 1.3 V and HER at -0.25 V. The stability of the prepared catalysts was evaluated by chronopotentiometry at a constant current density of 10 mA cm$^{-2.}$ To prepare the electrode, the catalyst materials were first grinded to be as a fine powder as possible. Then the catalyst ink was prepared in the same proportions as before and dispersed with an ultrasonic probe. Next, an appropriate amount of catalyst ink was evenly dripped onto both sides of the dried carbon paper, drying naturally. The ink was then dried in an oven at 60°C for one hour. The carbon paper was immersed in electrolytes for 12 hours before test. To estimate the electrochemically active surface areas (ECSAs), electrochemical bilayers were tested by CVs at different scan rates (20, 40, 60, 80 and 100 mV s^{-1}) in a potential window of 0.9 to 1.0 V versus RHE Capacitance (C_{dl}).

For the overall water splitting test, a two-electrode system in the 0.5 M H_2SO_4 aqueous electrolyte was deployed. Carbon paper with a size of 1 cm × 1 cm was used as the cathode and anode for HER and OER, respectively. Polarization curves were collected in the range of 1 to 2 V with a scan rate of 5 mV s^{-1}. Durability tests of bulk water splitting were recorded using chronopotentiometry at a constant current density of 10 mA cm^{-2}.

Theoretical Calculation: The simulation of the catalysts was calculated using spin-polarized density functional theory (DFT) and implemented using DMol^3 program. The pw91 correlation functional within the generalized gradient approximation (GGA) and the double numerical plus polarization (DNP) basis set were adopted for the calculations. A vacuum space of 15Å was used to avoid interactions between adjacent layers. K-point grid was set as 3*3*1 in geometry optimizations while 6*6*1 was set for the density of states.
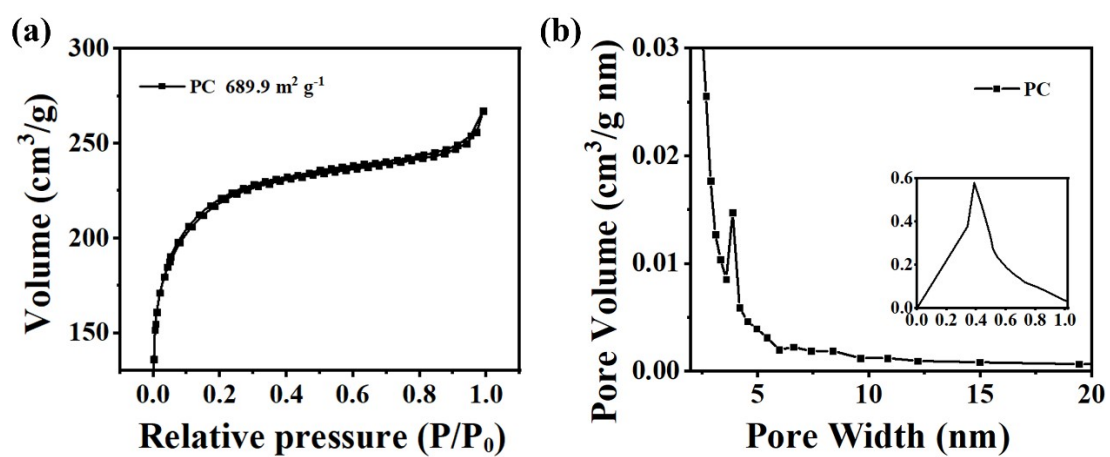
Figure S1 (a) N$_2$ adsorption-desorption isotherms and (b) pore size distribution curves (the inset shows the size distribution of micropores) of PC.
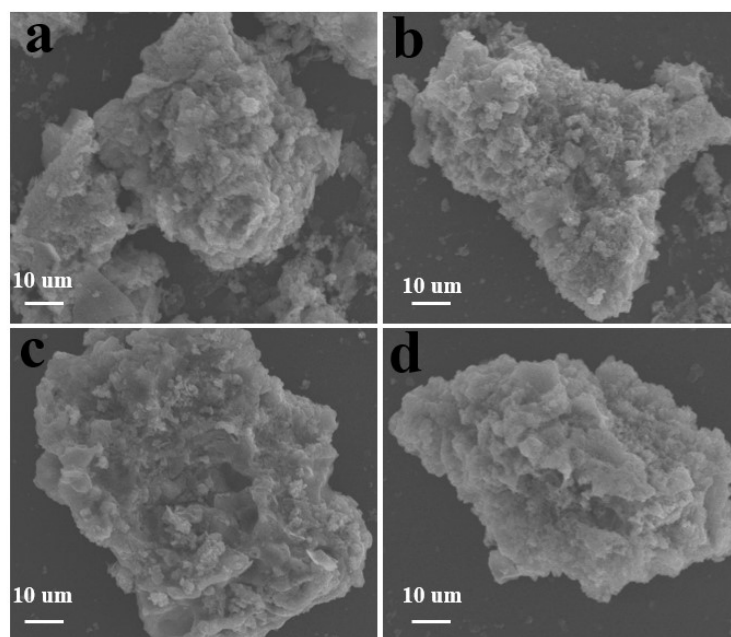
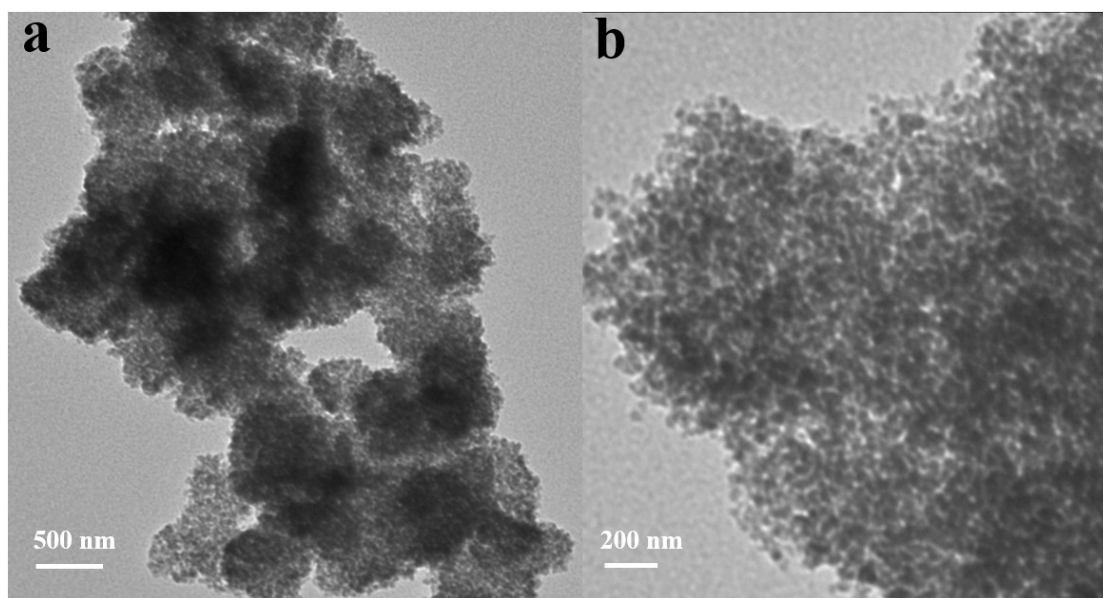**Figure S2** The SEM images of (a) RuO$_2$ NPS; (b) RuO$_2$/PC-1; (c) RuO$_2$/PC-0.4 and (d) RuO$_2$/PC-0.25.

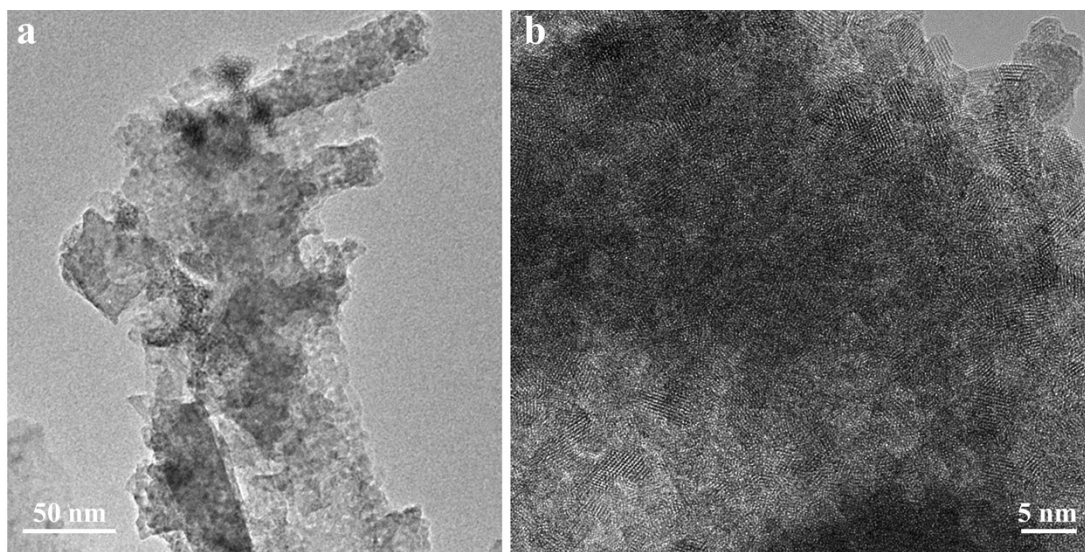**Figure S3** The TEM images of RuO$_2$ NPS.

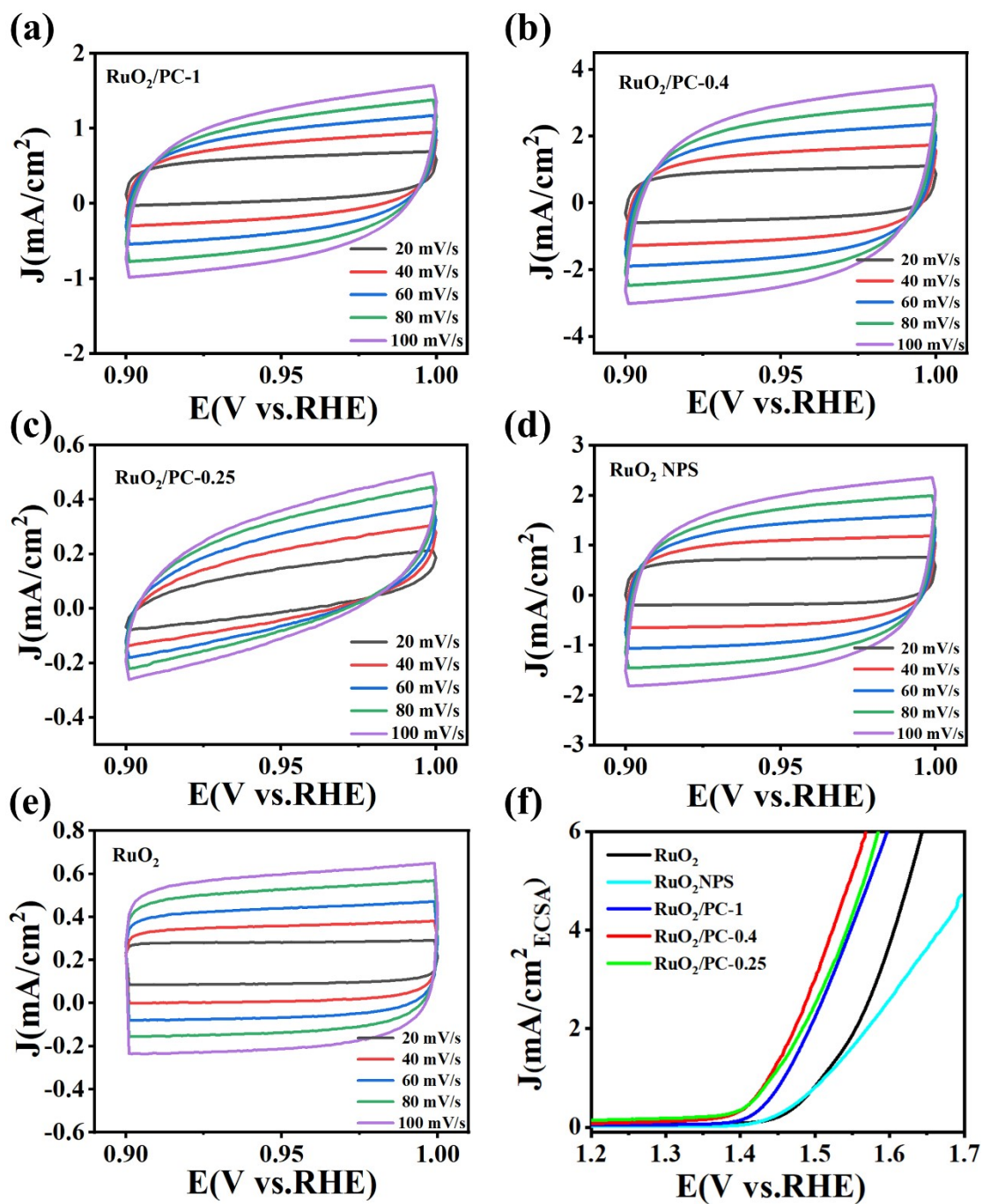**Figure S4** The TEM images of RuO_2/PC-0.4.

Figure S5 (a-e) Cyclic voltammograms in 0.5 M H_2SO_4 at various scan rates of 20, 40, 60, 80, and 100 mV s^{-1} in the voltage range of 0.9-1.0 V (vs. RHE). (f) OER polarization curves in 0.5 M H_2SO_4 normalized by their respective ECSA.
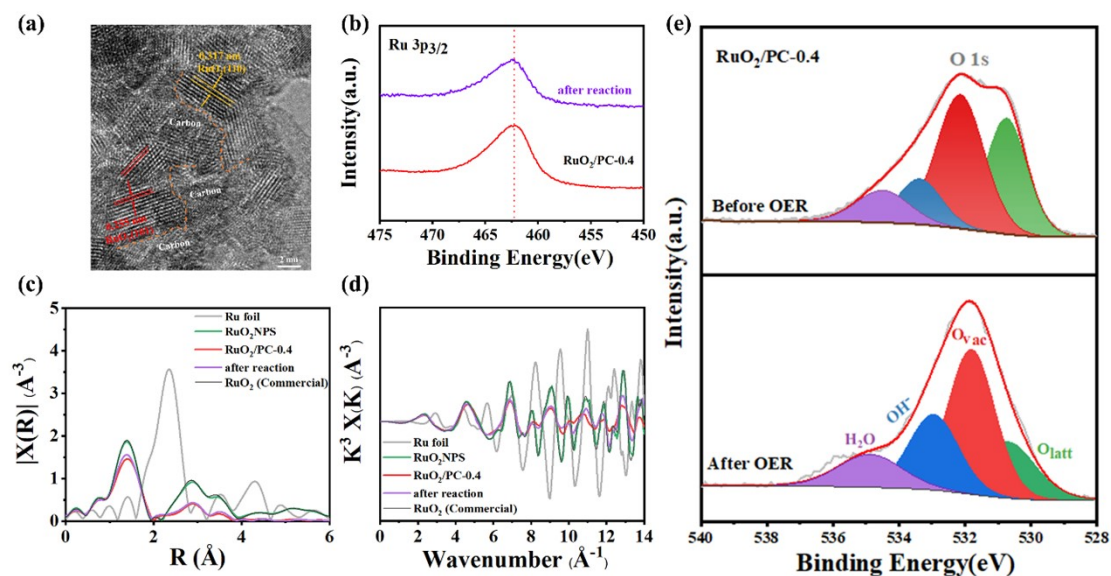
Figure S6 (a) HRTEM image of RuO_2/PC-0.4 catalyst after OER electrocatalysis for 24h. (b) XPS scans of Ru $3p_{3/2}$ in RuO_2/PC-0.4 catalyst before and after OER reaction for 24h. (c) EXAFS spectra of Ru foil, RuO_2NPS, commercial RuO_2 and RuO_2/PC-0.4 catalyst before and after OER electrocatalysis for the Ru K edge, and (d) Fourier transform of the EXAFS spectra in k spaces. (e) O 1s XPS measurement spectra of RuO_2/PC-0.4 catalyst before and after OER reaction.

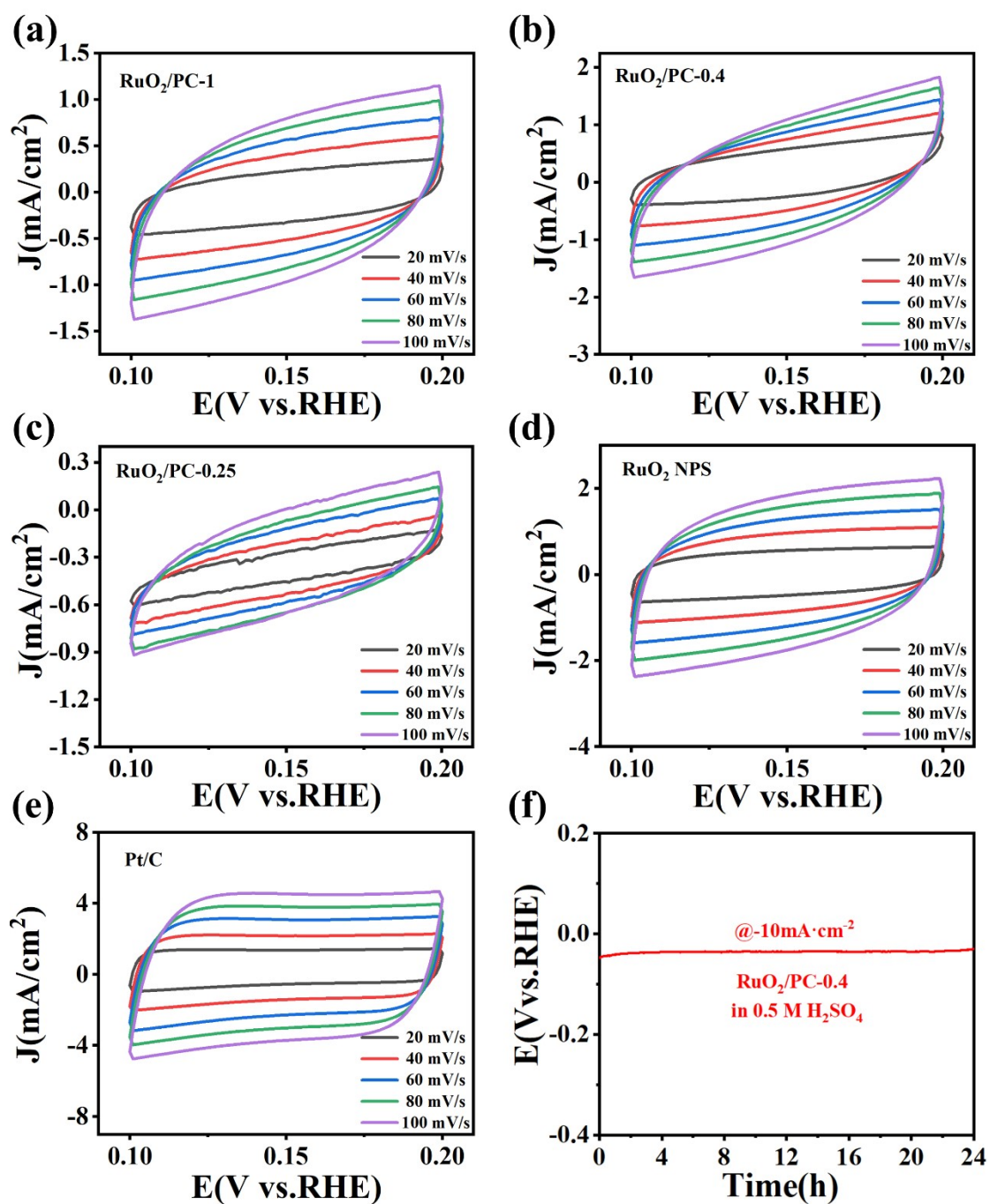**Figure S7** (a-e) Cyclic voltammograms in 0.5 M H_2SO_4 at various scan rates of 20, 40, 60, 80, and 100 mV s^{-1} in the voltage range of 0.1-0.2 V (vs. RHE). (f) Chronopotentiometry test of the RuO_2/PC-0.4 at -10 mA cm^{-2} in 0.5 M H_2SO_4.

(a) RuO₂ (110)

1: d-band: -3.52 eV   2: d-band: -3.22 eV

(b) GR-RuO₂ (110)

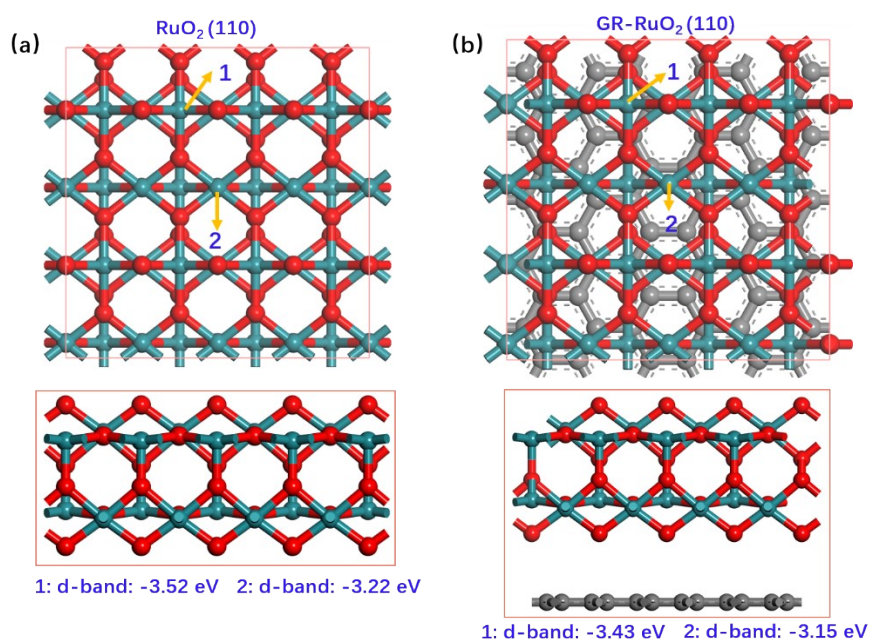1: d-band: -3.43 eV   2: d-band: -3.15 eV

Figure S8. Theoretical stimulation of the d-band center of Ru atoms in the two layers of RuO$_2$ without (a) and with (b) the substrate of one layer of graphene (GR).
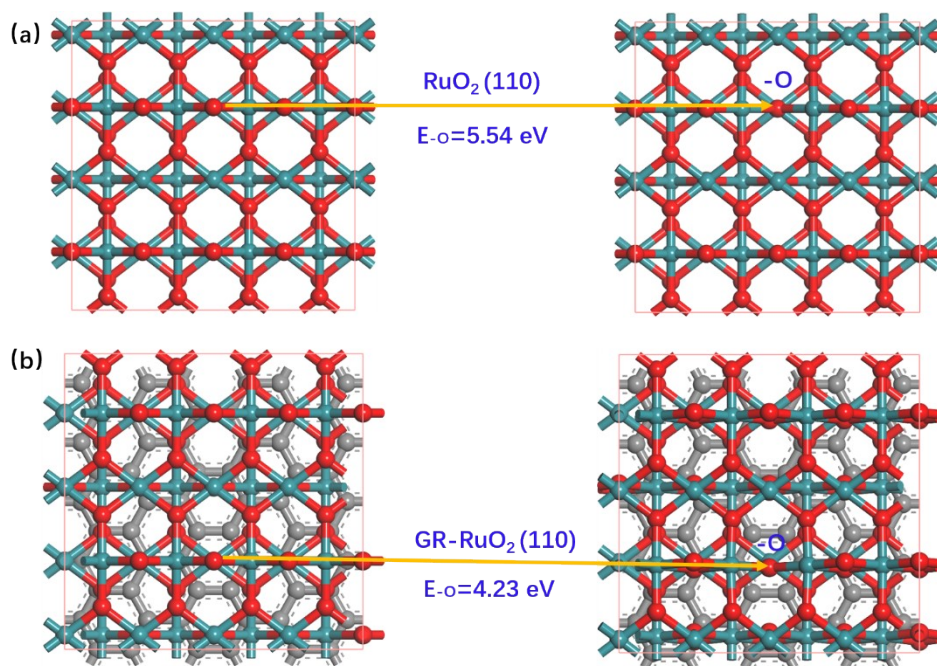
Figure S9. Theoretical stimulation of the oxygen vacancy formation energy (E_{-O}) of two layers of RuO_2 without (a) and with (b) the substrate of one layer of graphene (GR).
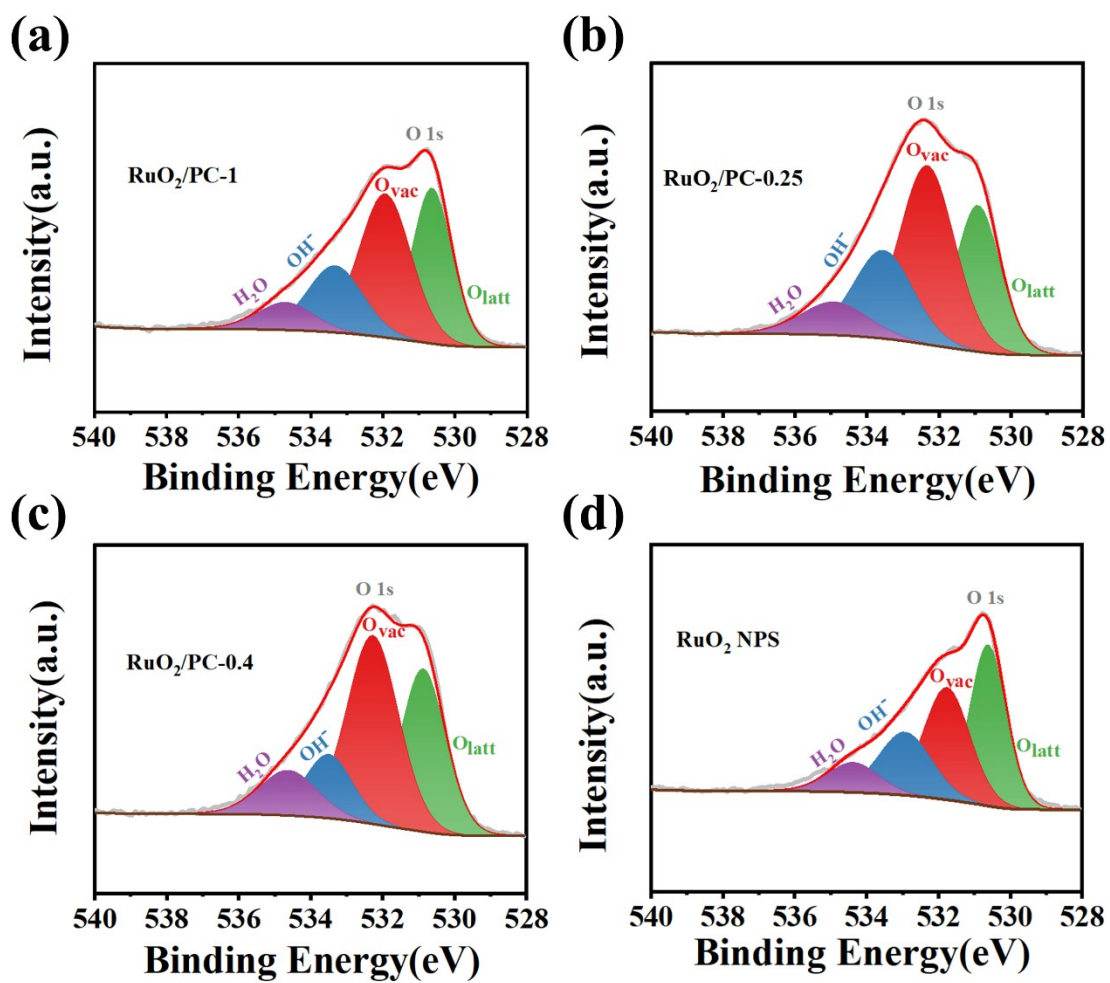
Figure S10 O 1s XPS measurement spectra of (a) RuO$_2$/PC -1, (b) RuO$_2$/PC -0.25, (c) RuO$_2$/PC - 0.4, (d) RuO$_2$ NPS

Table S1. Grain sizes of the as-prepared samples based on Scherrer formular*.

Sample	Average Crystallite, D (nm)
RuO$_2$/PC-0.25	3.10
RuO$_2$/PC-0.4	3.41
RuO$_2$/PC-1	3.44
RuO$_2$ NPS	3.52

$$* D = \frac{K\,\gamma}{B\,cos\theta}$$

Where D is the average thickness of the grain perpendicular to the direction of the grain surface (nm); γ is the X-ray wavelength, 0.154056 nm; θ is the Bragg diffraction angle. K is the Scherrer constant, here in the present work, B is adopted from the half height width of the diffraction peak, then K=0.89.

Table S2. ICP-OES results of RuO_2/PC-1，RuO_2/PC-0.4 and RuO_2/PC-0.25.

Sample	Ru content (wt%)
RuO_2/PC-1	8.4%
RuO_2/PC-0.4	6.4%
RuO_2/PC-0.25	4.4%

Table S3. Nitrogen adsorption/desorption measurement results for all samples.

Catalyst	BET Surface Area (m² g⁻¹)	Pore Volume （cm³ g⁻¹）	Pore Size （nm）
RuO₂/PC-1	194.3	0.37	9.11
RuO₂/PC-0.4	178.8	0.28	9.94
RuO₂/PC-0.25	167.5	0.31	15.67
PC	689.9	0.41	3.55

Table S4. Equivalent circuit fitting parameters for OER testing of all samples

Catalysts	Rs (Ω)	Rct (Ω)	CPE (mF)
RuO_2/PC-1	1.35	3.39	0.59
RuO_2/PC-0.4	1.25	2.12	0.66
RuO_2/PC-0.25	1.27	13.46	0.63
RuO_2	1.29	24.63	0.78
RuO_2 NPS	1.65	2.60	0.68

Table S5. Comparison of OER activity in acidic medium of the recently reported catalysts.

Catalysts	Electrolyte	Overpotential [mV] at 10 mA cm^{-2}	Reference
RuO$_2$/PC-0.4	0.5 M H$_2$SO$_4$	181	This work
Ir wavy nanowires	0.5 M HClO$_4$	270	[1]
Ir$_6$Ag$_9$ nanotubes	0.5 M H$_2$SO$_4$	285	[2]
IrCoNi PHNCs	0.1 M HClO$_4$	303	[3]
P-PNRO/C	0.1 M HClO$_4$	239	[4]
Ultrafine defective RuO2	0.5 M HClO$_4$	179	[5]
Branched Pd–Ru	0.1 M HClO$_4$	225	[6]
NaRuO$_2$ nanosheets	0.1 M HClO$_4$	255	[7]
Co$_2$TiO$_4$	0.5 M H$_2$SO$_4$	513	[8]
Amino-HNC	0.5 M H$_2$SO$_4$	281	[9]
N-doped graphite/carbon black	0.5 M H$_2$SO$_4$	470	[10]
C$_{60}$–SWCNTs	0.5 M H$_2$SO$_4$	400	[11]
Mesoporous Ir nanosheets	0.5 M H$_2$SO$_4$	240	[12]
IrNi$_2$–PE (H$^+$)	0.05 M H$_2$SO$_4$	315	[13]

Table S6. Equivalent circuit fitting parameters for HER testing of all samples

Catalysts	Rs (Ω)	Rct (Ω)	CPE (mF)
RuO$_2$/PC-1	1.16	31.82	0.48
RuO$_2$/PC-0.4	1.34	30.05	0.61
RuO$_2$/PC-0.25	1.01	29.86	0.51
Pt/C	1.16	0.28	0.50
RuO$_2$ NPS	1.84	45.33	0.77

Table S7. The XPS data of O 1s in all the as-synthesized catalysts and RuO_2/PC-0.4 catalyst after OER.

Catalysts	O_{latt} (%)	O_{vac} (%)	OH^- (%)	H_2O (%)
RuO_2/PC-1	50.8	32.2	13.4	3.6
RuO_2/PC-0.4	34.3	46.5	16.3	2.9
RuO_2/PC-0.25	27.6	44.7	22.6	5.1
RuO_2 NPS	58.9	28.4	10.6	2.1
RuO_2/PC-0.4 (after OER)	16.6	45.6	29.2	8.6

References：

[1] L. Fu, F. Yang, G. Cheng, W. Luo, *Nano.* 2018, **10**, 1892.

[2] M. Zhu, Q. Shao, Y. Qian, X. Huang, *Nano. Energy* 2019, **56**, 2211.

[3] J. Feng, F. Lv, W. Zhang, P. Li, K. Wang, C. Yang, B. Wang, Y. Yang, J. Zhou, F. Lin, G.C. Wang, S. Guo, *Adv. Mater.* 2017, **29**, 1703798.

[4] A. Oh, H. Y. Kim, H. Baik, B. Kim, N. K. Chaudhari, S. H. Joo, K. Lee, *Adv. Mater.* 2019, **31**, 1805546.

[5] R. Ge, L. Li, J. Su, Y. Lin, Z. Tian, L. Chen, *Adv. Energy Mater.* 2019, **9**, 1901313.

[6] L. Gloag, T.M. Benedetti, S. Cheong, C.E. Marjo, J. J. Gooding, R.D. Tilley, *J. Am. Chem. Soc.* 2018, **140**, 12760.

[7] S. Laha, Y. Lee, F. Podjaski, D. Weber, V. Duppel, L. M. Schoop, F. Pielnhofer, C. Scheurer, K. Müller, U. Starke, K. Reuter, B. V. Lotsch, *Adv. Energy Mater.* 2019, **9**, 1803795.

[8] S. Anantharaj, K. Karthick, S. Kundu, *Inorg. Chem.* 2019, **58**, 8570.

[9] X. Zhao, H. Su, W. Cheng, H. Zhang, W. Che, F. Tang, Q. Liu, *ACS Appl. Mater. Interfaces* 2019, **11**, 34854.

[10] R. Gao, Q. Dai, F. Du, D. Yan, L. Dai, *J. Am. Chem. Soc.* 2019, **141**, 11658.

[11] B. Jiang, Y. Guo, J. Kim, A. E. Whitten, K. Wood, K. Kani, A. E. Rowan, J. Henzie, Y. Yamauchi, *J. Am. Chem. Soc.* 2018, **140**, 12434.

[12] Y. Pi, Q. Shao, X. Zhu, X. Huang, *ACS Nano.* 2018, **12**, 7371.